Supporting Information

A Combined Experimental and Theoretical Study of Optical Rotatory Dispersion for (*R*)-Glycidyl Methyl Ether in Aqueous Solution

Franco Egidi[1], Tommaso Giovannini[1], Gianluca Del Frate[1], Paul M. Lemler[2],
Patrick H. Vaccaro*[2], and Chiara Cappelli†[1]

[1]Scuola Normale Superiore, Piazza dei Cavalieri 7, 56126 Pisa, Italy
[2]Department of Chemistry, Yale University, 225 Prospect Street, New Haven, CT
06520-8107 USA

September 28, 2018

*patrick.vaccaro@yale.edu
†chiara.cappelli@sns.it

1 Concentration-Dependent Experimental Measurements

Values of specific rotation, $[\alpha]_\lambda^T$ (in $\deg\,\mathrm{dm}^{-1}(\mathrm{g/mL})^{-1}$ with error bars representing one standard-deviation uncertainties), measured for ambient aqueous solutions of R-GME are plotted in Figure 1 as a function of solute concentration, C, to discern possible aggregation effects. The results obtained for each wavelength display a linear scaling with C (as highlighted by superimposed dashed lines which follow from least-squares regressions to a linear functional form), thereby enabling the intrinsic solvated response to be extracted from attendant ($C = 0$) intercepts. In keeping with the presumed absence of strong solute-solute coupling, the corresponding slopes for data acquired at 589.30, 578.39, 546.07, and 436.83 nm were statistically zero (uncertainties 2–20 times larger than their values), while barely significant slope parameters of $(2.4 \pm 1.1) \times 10^2$ and $(1.5 \pm 1.2) \times 10^2\,\deg\,\mathrm{dm}^{-1}(\mathrm{g/mL})^{-2}$ were determined from the 365.02 and 302.15 nm analyses, respectively. Experiments performed with 253.65 nm excitation revealed a specific rotation of $52.7 \pm 2.4\,\deg\,\mathrm{dm}^{-1}(\mathrm{g/mL})^{-1}$, however the limited transmission of such deep-ultraviolet light through aqueous samples of R-GME (1 dm pathlength) prohibited a systematic concentration study and lessened the overall confidence of this finding.
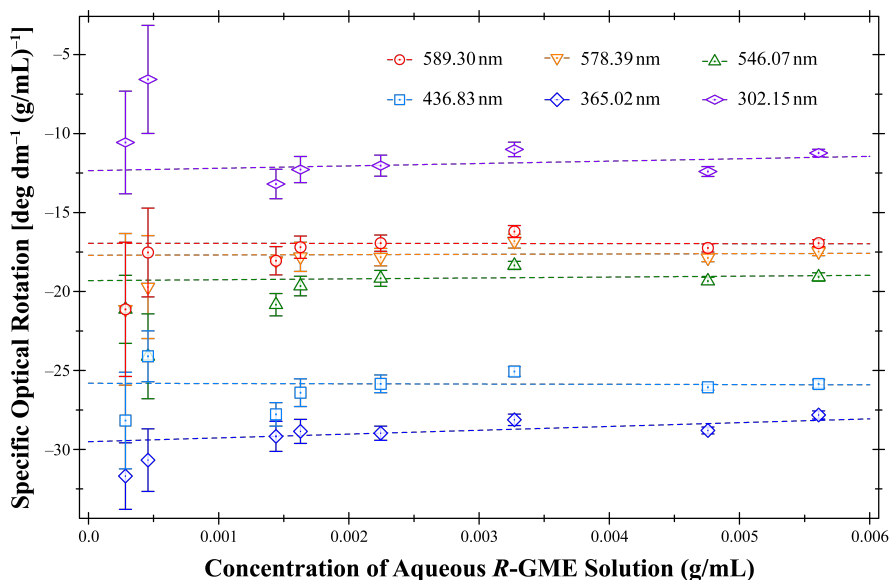

Figure 1: **Concentration Dependence of Optical Activity for Aqueous R-GME.**

2 Excitation energies for different electronic structure methods

Calculated ORD curves are expected to diverge as the wavelength approaches the location of the poles in the response functions corresponding to each method. In figure 2 we report a graphical representation of the first excitation energy for several different functionals as well as CCSD, using the aug-cc-pVDZ basis set, and for each conformer of R-GME optimized at the aug-cc-pVDZ level of theory. It can be observed from the figure that most functionals yield excitation energies that range from 6 to 7 eV, and some yield values that are closer to the CCSD results compared to others. This information alone is not enough to establish weather a given computed

ORD will agree more with CCSD results, since other excited states also play an important role in determining the quantitative value of the computed property, and while the energy gives the location of the pole the transition magnetic and electric dipole moments are also needed in order to evaluate the full weight that each excited state carries in the sum-over-state expression for the ORD. These values, however, tell us at which wavelength the computed ORD is expected to diverge and therefore give results that are no longer comparable with the experimental observable, unless a method that explicitly includes excite-state lifetimes in the calculation is employed when solving the response equations.

3 Calculated Dispersive Optical Activity of R-GME

Table 1 reports specific optical rotation (SOR) values for the nine conformers of R-GME in water as predicted with 11 different functionals and the aug-cc-pVDZ basis set. Solvent effects are accounted for using the polarizable continuum model (PCM). The equilibrium geometries employed in these calculations were optimized at the B3LYP/aug-cc-pVDZ/PCM level of theory.
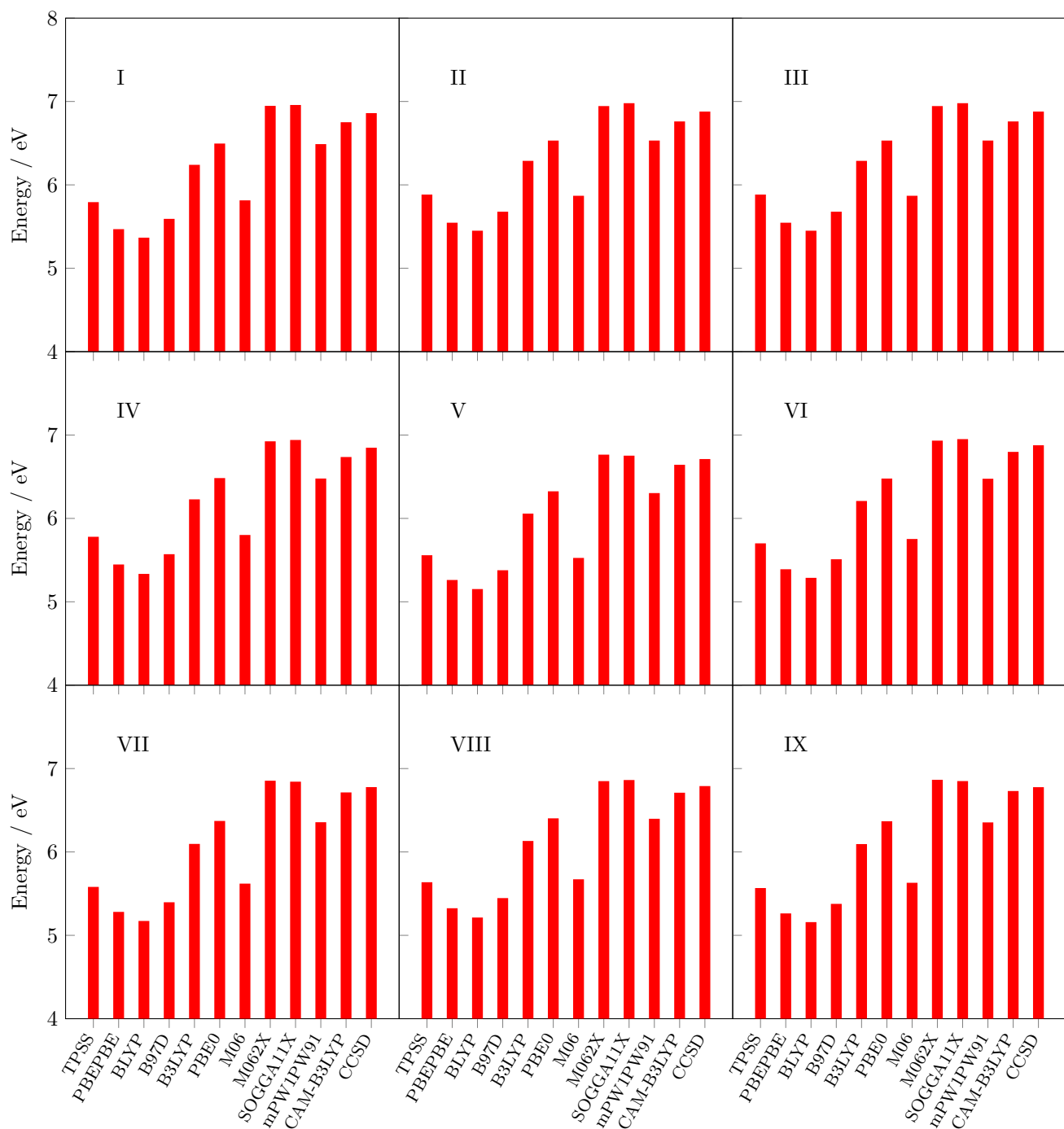
Figure 2: Excitation energies of the *R*-GME conformers in vacuo computed using different methods and the aug-cc-pVDZ basis set, at the B3LYP/aug-cc-pVDZ optimized geometries.

254.65 nm

Conf	TPSSTPSS	PBEPBE	BLYP	B97D	B3LYP	PBE0	M06	M06-2X	SOGGA11X	mPW1PW91	CAM-B3LYP
I	729.93	1160.02	1328.13	864.89	355.15	225.08	335.81	79.16	90.92	190.92	165.64
II	436.99	561.70	699.03	479.13	291.63	248.36	267.93	218.38	233.20	244.81	297.14
III	-104.98	-243.00	-192.76	-97.78	23.19	24.12	-35.84	77.03	83.52	18.59	6.73
IV	1267.71	1678.50	1737.06	1445.71	904.53	758.26	938.07	601.33	620.24	731.80	661.33
V	2747.19	6397.20	9241.98	3891.82	481.38	-2.72	1289.38	-448.48	-354.84	-19.76	-152.18
VI	-755.12	-966.00	-977.45	-816.72	-502.35	-447.98	-688.02	-393.30	-351.10	-424.66	-284.68
VII	1136.28	2832.70	3922.56	1738.99	-284.68	-620.16	11.31	-936.24	-837.84	-633.97	-727.79
VIII	1937.21	2091.57	2017.87	1974.11	1698.01	1667.66	1695.41	1624.05	1532.85	1639.30	1568.44
IX	1715.83	1184.27	687.82	1632.32	2169.12	2219.25	2002.52	2252.01	2112.75	2198.91	2057.76

302.15 nm

Conf	TPSSTPSS	PBEPBE	BLYP	B97D	B3LYP	PBE0	M06	M06-2X	SOGGA11X	mPW1PW91	CAM-B3LYP
I	152.03	243.33	285.88	181.12	59.37	17.11	40.31	-34.20	-21.82	2.58	1.43
II	135.85	167.05	186.81	148.15	119.02	111.41	100.18	100.12	111.39	107.97	138.51
III	-58.87	-87.47	-57.66	-55.13	-17.48	-15.59	-29.75	11.41	19.30	-19.04	-25.56
IV	530.88	679.96	710.72	600.63	415.70	361.14	417.37	294.63	311.25	347.60	321.19
V	49.80	417.51	629.73	195.84	-225.40	-341.11	-161.51	-464.83	-401.14	-346.98	-331.95
VI	-347.61	-425.71	-427.13	-362.40	-245.47	-224.87	-310.98	-206.47	-186.85	-214.81	-149.46
VII	-366.06	-134.45	11.88	-271.23	-583.36	-668.88	-540.52	-737.48	-684.31	-670.46	-654.94
VIII	1137.25	1222.84	1195.81	1159.89	1029.98	1016.65	1026.91	985.01	942.72	1001.88	955.96
IX	1462.42	1502.77	1440.80	1509.25	1442.44	1432.31	1407.03	1401.38	1333.68	1417.56	1309.64

355.00 nm

Conf	TPSSTPSS	PBEPBE	BLYP	B97D	B3LYP	PBE0	M06	M06-2X	SOGGA11X	mPW1PW91	CAM-B3LYP
I	27.55	58.44	77.56	37.39	-7.39	-26.31	-18.56	-50.14	-40.63	-34.08	-31.53
II	61.08	74.85	79.63	67.84	62.45	61.61	50.74	55.28	63.76	59.14	78.20
III	-48.46	-63.81	-49.28	-47.92	-25.85	-23.12	-29.40	-5.93	0.56	-25.25	-29.09
IV	285.81	359.05	371.48	321.86	234.07	206.99	232.15	170.95	183.61	198.98	185.97
V	-201.74	-96.01	-25.81	-151.67	-264.13	-310.35	-256.21	-362.52	-319.55	-312.85	-286.35
VI	-199.86	-237.00	-234.87	-203.87	-144.40	-134.29	-177.15	-126.61	-115.20	-128.84	-91.30
VII	-441.64	-379.00	-321.98	-410.98	-490.43	-524.02	-473.29	-540.58	-508.45	-523.13	-498.04
VIII	744.96	794.08	776.06	758.10	682.43	675.35	679.21	652.73	629.59	666.41	635.24
IX	1024.76	1079.32	1053.88	1060.19	976.55	964.74	957.56	933.89	895.68	954.69	881.05

Table 1: SOR for each conformer of aqueous *R*-GME computed with different functionals, the aug-cc-pVDZ basis set, and the polarizable-continuum model of solvation.

365.02 nm

Conf	TPSSTPSS	PBEPBE	BLYP	B97D	B3LYP	PBE0	M06	M06-2X	SOGGA11X	mPW1PW91	CAM-B3LYP
I	17.85	43.92	60.97	26.15	-12.24	-28.96	-22.39	-50.11	-41.09	-36.01	-33.29
II	54.10	66.37	70.13	60.33	56.52	56.15	45.74	50.33	58.38	53.84	71.48
III	-46.65	-60.77	-47.80	-46.37	-25.97	-23.23	-28.79	-7.22	-1.01	-25.19	-28.72
IV	259.77	325.61	336.41	292.40	213.91	189.58	211.91	156.81	168.82	182.22	170.56
V	-210.07	-121.61	-60.87	-166.86	-258.65	-299.02	-253.46	-344.82	-304.65	-301.19	-274.94
VI	-183.41	-216.57	-214.29	-186.55	-132.84	-123.78	-162.37	-117.12	-106.63	-118.83	-84.40
VII	-432.24	-381.20	-330.92	-406.23	-469.42	-498.59	-453.98	-511.07	-481.47	-497.55	-472.67
VIII	695.26	740.30	723.49	707.29	637.66	631.24	634.52	609.91	588.90	623.00	593.79
IX	961.89	1014.48	991.77	994.98	914.14	902.76	896.56	872.94	838.07	893.36	824.49

436.83 nm

Conf	TPSSTPSS	PBEPBE	BLYP	B97D	B3LYP	PBE0	M06	M06-2X	SOGGA11X	mPW1PW91	CAM-B3LYP
I	-11.80	-2.24	6.77	-8.75	-24.54	-32.78	-30.15	-43.39	-37.07	-36.77	-34.04
II	27.06	33.63	34.29	31.02	31.69	32.63	25.19	28.97	34.71	31.08	42.10
III	-35.44	-44.35	-37.63	-35.97	-23.09	-20.66	-23.41	-10.25	-5.69	-21.85	-24.02
IV	149.17	185.16	190.02	167.62	126.06	112.92	124.33	93.99	102.49	108.45	102.24
V	-197.44	-164.19	-135.60	-177.65	-205.03	-224.01	-206.08	-245.93	-219.53	-224.97	-203.74
VI	-110.92	-128.29	-126.00	-111.25	-81.15	-76.35	-97.61	-73.53	-67.13	-73.51	-52.80
VII	-340.35	-325.66	-299.81	-329.81	-342.72	-355.88	-333.34	-355.47	-337.40	-354.55	-334.25
VIII	456.17	483.26	472.33	463.31	420.51	416.91	418.09	402.20	390.36	411.80	392.31
IX	644.35	681.82	669.22	665.39	606.50	598.36	594.95	575.97	555.75	592.19	546.89

546.07 nm

Conf	TPSSTPSS	PBEPBE	BLYP	B97D	B3LYP	PBE0	M06	M06-2X	SOGGA11X	mPW1PW91	CAM-B3LYP
I	-17.03	-14.03	-9.38	-16.06	-22.10	-25.96	-24.91	-30.99	-27.03	-28.10	-26.10
II	12.94	16.42	16.22	15.33	16.78	17.80	13.19	15.61	19.29	16.86	23.22
III	-23.79	-29.12	-25.83	-24.42	-16.84	-15.07	-16.35	-8.82	-5.86	-15.75	-16.99
IV	80.83	99.71	101.80	90.77	69.61	62.86	68.54	52.53	57.94	60.33	57.19
V	-141.33	-128.87	-114.98	-132.01	-138.07	-146.81	-139.50	-156.92	-141.08	-147.19	-133.03
VI	-62.94	-71.64	-69.97	-62.44	-46.31	-43.91	-55.13	-42.89	-39.22	-42.38	-30.70
VII	-227.50	-224.73	-211.33	-223.19	-221.33	-227.09	-215.48	-223.40	-213.21	-226.01	-212.32
VIII	275.37	290.64	284.13	279.31	254.68	252.78	253.08	243.57	237.37	249.84	237.94
IX	392.63	415.38	408.37	404.62	367.99	363.05	360.78	348.49	337.59	359.35	332.17

Table 1: cont. **SOR for each conformer of aqueous *R*-GME computed with different functionals, the aug-cc-pVDZ basis set, and the polarizable-continuum model of solvation.**

6

578.39 nm

Conf	TPSSTPSS	PBEPBE	BLYP	B97D	B3LYP	PBE0	M06	M06-2X	SOGGA11X	mPW1PW91	CAM-B3LYP
I	-16.53	-14.27	-10.28	-15.80	-20.63	-23.88	-23.02	-28.11	-24.59	-25.72	-23.90
II	10.92	13.93	13.67	13.03	14.45	15.42	11.34	13.48	16.76	14.59	20.14
III	-21.38	-26.09	-23.30	-21.98	-15.33	-13.72	-14.78	-8.21	-5.56	-14.31	-15.40
IV	69.92	86.16	87.88	78.51	60.42	54.63	59.48	45.69	50.50	52.43	49.75
V	-127.89	-117.86	-106.04	-119.99	-123.98	-131.31	-125.29	-139.78	-125.83	-131.62	-118.94
VI	-54.93	-62.34	-60.83	-54.39	-40.46	-38.41	-48.08	-37.61	-34.41	-37.09	-26.90
VII	-203.98	-202.34	-190.80	-200.44	-197.51	-202.28	-192.28	-198.52	-189.65	-201.29	-189.00
VIII	243.03	256.33	250.60	246.44	224.89	223.25	223.46	215.07	209.75	220.68	210.16
IX	346.92	366.94	360.83	357.36	324.97	320.62	318.55	307.63	298.22	317.36	293.42

589.30 nm

Conf	TPSSTPSS	PBEPBE	BLYP	B97D	B3LYP	PBE0	M06	M06-2X	SOGGA11X	mPW1PW91	CAM-B3LYP
I	-16.30	-14.24	-10.44	-15.63	-20.14	-23.21	-22.40	-27.21	-23.83	-24.97	-23.21
II	10.35	13.22	12.95	12.38	13.78	14.72	10.80	12.86	16.02	13.93	19.25
III	-20.65	-25.17	-22.52	-21.24	-14.85	-13.30	-14.30	-8.00	-5.46	-13.86	-14.90
IV	66.75	82.23	83.85	74.95	57.74	52.23	56.84	43.69	48.32	50.12	47.58
V	-123.71	-114.35	-103.12	-116.22	-119.67	-126.61	-120.94	-134.62	-121.22	-126.90	-114.67
VI	-52.58	-59.63	-58.17	-52.04	-38.74	-36.80	-46.01	-36.06	-32.99	-35.53	-25.79
VII	-196.82	-195.46	-184.45	-193.48	-190.31	-194.81	-185.27	-191.06	-182.57	-193.84	-181.99
VIII	233.42	246.14	240.64	236.67	216.03	214.47	214.65	206.59	201.53	212.01	201.90
IX	333.30	352.52	346.66	343.30	312.17	307.99	305.99	295.48	286.51	304.87	281.89

633.00 nm

Conf	TPSSTPSS	PBEPBE	BLYP	B97D	B3LYP	PBE0	M06	M06-2X	SOGGA11X	mPW1PW91	CAM-B3LYP
I	-15.23	-13.78	-10.61	-14.75	-18.22	-20.72	-20.08	-23.98	-21.06	-22.19	-20.64
II	8.46	10.88	10.58	10.21	11.52	12.38	9.01	10.78	13.52	11.69	16.22
III	-18.04	-21.92	-19.75	-18.59	-13.14	-11.77	-12.57	-7.23	-5.02	-12.24	-13.13
IV	56.06	69.00	70.30	62.96	48.66	44.08	47.90	36.90	40.91	42.30	40.19
V	-108.68	-101.41	-92.12	-102.51	-104.40	-110.05	-105.51	-116.55	-105.08	-110.27	-99.64
VI	-44.59	-50.42	-49.13	-44.04	-32.88	-31.28	-38.99	-30.73	-28.12	-30.21	-21.96
VII	-171.44	-170.91	-161.69	-168.79	-165.04	-168.65	-160.65	-165.02	-157.84	-167.79	-157.47
VIII	200.21	210.99	206.28	202.95	185.40	184.10	184.20	177.30	173.09	182.00	173.32
IX	286.19	302.60	297.62	294.63	267.91	264.34	262.56	253.49	245.98	261.67	242.00

Table 1: cont. **SOR for each conformer of aqueous *R*-GME computed with different functionals, the aug-cc-pVDZ basis set, and the polarizable-continuum model of solvation.**